AAPS PharmSciTech, Vol. 15, No. 6, December 2014 (© 2014)
DOI: 10.1208/s12249-014-0165-0

Research Article

Theme: Translational Application of Nano Delivery Systems: Emerging Cancer Therapy
Guest Editors: Mahavir B. Chougule and Chalet Tan

Brain-Targeted Delivery of Docetaxel by Glutathione-Coated Nanoparticles for Brain Cancer

Aditya Grover,[1] Anjali Hirani,[1] Yashwant Pathak,[1] and Vijaykumar Sutariya[1,2]

Received 22 November 2013; accepted 28 May 2014; published online 19 August 2014

Abstract. Gliomas are some of the most aggressive types of cancers but the blood–brain barrier acts as an obstacle to therapeutic intervention in brain-related diseases. The blood–brain barrier blocks the permeation of potentially toxic compounds into neural tissue through the interactions of brain endothelial cells with glial cells (astrocytes and pericytes) which induce the formation of tight junctions in endothelial cells lining the blood capillaries. In the present study, we characterize a glutathione-coated docetaxel-loaded PEG-PLGA nanoparticle, show its *in vitro* drug release data along with cytotoxicity data in C6 and RG2 cells, and investigate its trans-blood–brain barrier permeation through the establishment of a Transwell cellular co-culture. We show that the docetaxel-loaded nanoparticle's size enables its trans-blood–brain barrier permeation; the nanoparticle exhibits a steady, sustained release of docetaxel; the drug is able to induce cell death in glioma models; and the glutathione-coated nanoparticle is able to permeate through the Transwell *in vitro* blood–brain barrier model.

KEY WORDS: blood–brain barrier; brain cancer; docetaxel; glutathione; nanoparticle.

INTRODUCTION

Docetaxel, also known as Taxotere®, is a compound modified from paclitaxel (Taxol®) at two chemical positions, thereby making it more water-soluble than its parent compound. Despite being used against a wide variety of cancers, there are a number of adverse effects associated with docetaxel, mainly associated with the solvent, polysorbate 80, used to administer the drug (1). In addition to adverse effects, there were reports that polysorbate 80 altered the pharmacokinetic profiles of the drug (2). These conditions greatly limit the applications of the drug in clinical settings. Given the therapeutic potential of docetaxel, its use as an antineoplastic agent in brain cancers could be considered. Phase II clinical studies currently administer the drug at a concentration of 80 mg/m^2 every 3 weeks (3). However, the blood–brain barrier (BBB) acts as an obstacle to its use against brain cancers.

The majority of brain tumors in adults are glioblastomas, making them the most common primary brain tumor (4,5). Astrocytomas represent one of three different histopathological subgroups of glioblastomas, and usually have between 60 and 70% rate of malignancy, the highest rate of the three (6). The dismal prognoses of astrocytomas is associated with its ability to infiltrate normal brain parenchyma, contributing to the 1-year life span following diagnosis experienced by most patients (6,7). This ability also enables astrocytomas to recur in tissues after resection, often in the same location and with a higher rate of malignancy (8). The C6 and RG2 rat astrocytoma and glioma cell lines were developed in an effort to better study this complicated disease, and have since become a great model by which to study gliomas (7,9–11).

Although brain cancers are some of the most aggressive and have the lowest prognosis rates, physiological constraints in the central nervous system (CNS) provide obstacles to brain-targeted therapeutics. The BBB is the interface between the brain's blood capillaries and neural tissue composed of the interactions between endothelial cells, astrocytes, and pericytes (12). Through the activities of certain transport proteins, some molecules, such as water- and lipid-soluble substances, are able to permeate across the BBB (13). The interactions of various cell types at the BBB induce the formation of tight junctions in endothelial cells lining the blood capillaries in the brain (12). These tight junctions, along with many specialized proteins, limit the permeation of large therapeutic compounds across the BBB and may even induce their breakdown (13). This provides for a rather formidable yet effective defense system against toxins that may enter the brain, but comes as a disadvantage when attempting to treat brain-related disorders (14).

In our efforts to hijack the transport mechanisms present at the BBB interface, we devised the development of a glutathione (GSH)-coated poly(ethylene glycol)ylated (PEGylated) poly-(lactide-co-glycolide) (PLGA) nanoparticle (NP) that encapsulates docetaxel to enhance its trans-BBB

[1] Department of Pharmaceutical Sciences, College of Pharmacy, University of South Florida, 12901 Bruce B. Downs Blvd. MDC 30, Tampa, Florida 33612-4749, USA.
[2] To whom correspondence should be addressed. (e-mail: vsutariy@health.usf.edu;)

permeability. GSH is an antioxidant found in many different tissues that protects against oxidative stress (15). GSH concentrations in the CNS are much higher than in other body tissues, with a CNS concentration of up to 3 mM (15,16). In addition, a large number of GSH receptors exist at the BBB interface (10,17). By coating the organic nanoparticles with GSH, there may be an increased transcytosis of the drug-encapsulated particle across the BBB, thereby making it a suitable vector for brain-targeted therapies. Utilizing existing GSH receptor mechanisms to induce the trans-BBB permeation of therapies would greatly affect a number of brain-related disorders apart from cancer, including depression, Parkinson's, and schizophrenia (14). We have previously shown that GSH-coated nanoparticles are able to encapsulate a number of anti-mitotic compounds (10,11). More importantly, we have also shown that GSH-coated coumarin nanoparticles injected peritoneally were able to permeate the BBB in C57BL/6 mice due to the high level of GSH transporters located in the brain (10).

The present study utilizes a Transwell co-culture system to simulate the BBB in an *in vitro* setting through co-culturing rat endothelial cells (RBE4) and astrocytic cells (C6) on either side of the Transwell permeable insert. The 0.4 μm permeable membrane of the Transwell model allows the cell media between the two cell lines to be shared without the physical transfer of cells (18), giving it the status of being considered the "gold standard modeling system" for such studies (19). Co-culturing endothelial cells with astrocytes helps to induce BBB-specific characteristics in the endothelial cells, such as an increased expression of tight junction and transport proteins (20,21). Such models are priceless for investigating the trans-BBB permeation of drug compounds to directly target brain tissue.

The present study is one of the first to characterize a docetaxel-loaded PEGylated PLGA NP for use against brain cancers. PEGylated PLGA NPs were used because of their controlled drug release, low toxicities, few side effects, federal approval, and biodegradability (10,11,22,23). In addition, conjugating the PLGA NPs with PEG increases its circulatory retention time by evading the reticuloendothelium system (RES) thereby considerably increasing the NPs' circulatory time (24), as PLGA nanoparticles are prone to uptake by macrophages (10,22,23).

In vitro BBB permeation data obtained by establishing a co-culture on Transwell inserts yielded data that supported the hypothesis that NPs coated with GSH would permeate the BBB better than the free drug solution.

MATERIALS AND METHODS

Materials

PEGylated PLGA (5050 DLG, mPEG 5000) was purchased from Lakeshore Biomaterials, Birmingham, AL, USA. Docetaxel was purchased from Biotang, Waltham, MA, USA. Glutathione (reduced) was purchased from Fisher BioReagents. Phosphate-buffered saline (PBS) solution was purchased from Cellgro (Corning Inc., NY, USA). Thiazolyl blue tetrazolium bromide (MTT reagent) was purchased from Sigma-Aldrich. Acetone and methanol were both purchased from Sigma-Aldrich.

Preparation of Glutathione-Coated PEGylated PLGA NP

PEGylated PLGA NPs entrapped docetaxel using a previously established protocol (10). Briefly, 3 mL of acetone was used to dissolve 120 mg of PEGylated PLGA polymer with 4 mg of docetaxel. The resulting solution was added dropwise to 10 mL of deionized water (stirred at 300 rpm at 40°C) to yield a 12 mg/mL polymer/water solution; the acetone was allowed to completely evaporate. The resulting NP suspension was centrifuged at 5,000 rpm for 10 min to collect the particles, decant the resultant drug solution, and replace it with fresh deionized water to make up a total of 10 mL NP suspension. GSH was coated onto the NPs using a previously reported method (10). Twenty milligrams of GSH was added to 1 mL of the final NP suspension to obtain 2% *w*/*v* GSH coating on the NPs. The NP suspension was allowed to sit at room temperature for 30 min to allow a maximal GSH coating.

Determination of Entrapment Efficiency

The determination of the NP's entrapment efficiency of the drug was determined by using a previously reported method (10). Briefly, 1 mL of docetaxel-loaded NPs were centrifuged at 10,000 rpm for 10 min. The supernatant was removed and replaced with 1 mL of methanol and stored at 4°C overnight. The supernatant of the methanol/NP solution was measured by UV spectroscopy at a wavelength of 231 nm (λ_{max}). The supernatant was analyzed and compared to an analyzed set of standard dilutions in methanol ($r^2=0.9971$). The entrapment efficiency was determined using the following equation:

$$Entrapment\ \ Efficiency = \frac{Actual\ \ drug\ \ concentration}{Theoretical\ \ drug\ \ concentration} \times 100$$

In Vitro Drug Release

The rate of docetaxel release from the nanoparticles was measured by adapting a previously-reported method (25). Briefly, 15 μM equivalent of the NP suspension was added to 10 mL of phosphate-buffered saline (PBS 1×) solution maintained at 40°C and stirring at 60 rpm. One-milliliter aliquots were removed at predetermined intervals and replaced with fresh PBS (1×) solution. Aliquots were analyzed using UV spectroscopy at a wavelength of 231 nm (λ_{max}) and compared to standard dilutions of docetaxel prepared in PBS (1×) ($r^2=0.9993$) to determine the percentage of drug released over 240 h (10 days). The experiment was carried out in triplicates ($n=3$).

Cell Culture

RG2 (rat glioblastoma) cells were purchased from ATCC (CRL-2433™). C6 (rat glioma) cells were purchased from ATCC (CCL-107™). RBE4 (rat brain endothelium) cells were gifted by Dr. Aschner (Vanderbilt University Medical Center, Nashville, TN, USA). Cell culture plates and flasks were purchased from Corning Inc. (Corning, NY, USA). Transwell permeable support inserts (no. 3460) were

purchased from Corning Inc. (Corning, NY, USA). Ham's F10 medium and MEM medium were purchased from Cellgro® (Corning Inc., NY, USA). One percent penicillin and streptomycin was purchased from Invitrogen. Fetal bovine serum (FBS) was purchased from Invitrogen (Grand Island, NY, USA). PBS solution was purchased from Cellgro (Corning Inc., NY, USA). Human recombinant diluted basic fibroblast growth factor was purchased from BD Biosciences (San Jose, CA, USA). Rat tail collagen I was purchased from BD Biosciences (San Jose, CA, USA).

MTT Assay

Cytotoxicity of docetaxel-free drug in solution, docetaxel NP, and GSH-coated docetaxel NP were tested by MTT assay in RG2 and C6 cell lines. Briefly, 5×10^4 cells of each cell line were plated in each well of a 24-well plate (Corning Inc., NY, USA) and allowed to incubate (37°C, 5% CO_2) for 24 h to achieve 70–90% confluency. After 24 h, each cell line was exposed to the following identical treatments: 5 μM free docetaxel drug solution, 5 μM docetaxel NP, 5 μM GSH-coated docetaxel NP, 10 μM free docetaxel drug solution, 10 μM docetaxel NP, and 10 μM GSH-coated docetaxel NP. Each treatment was carried out in triplicates ($n=3$). Cells were treated for 24 h. After 24 h of treatment, the cell medium was aspirated and 500 μL MTT reagent solution (1 mg/mL) was added to each well. Cells were allowed to incubate (37°C, 5% CO_2) for 4 h. After 4 h, the MTT reagent solution was aspirated and 1 mL DMSO was added to each well. Both plates were allowed to gently shake for 10 min. The plates were read by the Synergy H4 plate reader (Biotek Industries Inc.) at absorbance of 570 nm.

In Vitro Blood–Brain Barrier Permeation Model

A Transwell model was established to investigate the BBB permeability of the docetaxel nanoparticles which was adapted from a previously reported method (26). Briefly, Transwell permeable supports with 0.4 μm porous membrane (Corning Inc., NY, USA) were purchased and both sides were coated with 0.1% rat tail collagen I (BD Biosciences™). C6 rat astrocytoma cells (ATCC®, CCL-107™) were seeded at the bottom of the support at 5×10^4 cells and allowed to adhere onto the collagen matrix for 24 h in incubator (37°C and 5% CO_2). After 24 h, 5×10^5 RBE4 rat brain endothelial cells were seeded to the inside of the support. Both cells were bathed in 2 mL of 1:1 mixture of Ham's F10:MEM media (Cellgro, Corning Inc., NY, USA) supplemented with 10% fetal bovine serum (FBS; Invitrogen, NY, USA), 1% penicillin and streptomycin (Invitrogen, NY, USA), and human recombinant diluted basic fibroblast growth factor (BD Biosciences, CA, USA); 1.5 mL was added to plate under the support to bathe the C6 cells and 0.5 mL media was added inside the support to bathe the RBE4 cells. Permeable supports bathed in media and seeded on both sides were allowed to incubate for 24 h before drug treatment. Five micromolar each of docetaxel-free drug in solution, docetaxel-loaded NP, and docetaxel-loaded 2% GSH-coated NPs were added inside of the support ($n=4$), and 100 μL samples of media were removed and replaced with fresh medium from under the support at predetermined time intervals over 48 h. The samples were analyzed by UV spectroscopy at a wavelength of 231 nm (λ_{max}).

Trans-Endothelial Electrical Resistance of the Transwell Model

The trans-endothelial electrical resistance (TEER) of the Transwell model was carried out to evaluate the model's effectiveness as a model of the BBB. TEER values were measured over 48 h, starting from 24 h after seeding the Transwell model with cells to allow confluency. TEER values were measured using the STX2 electrode and EVOM^2 epithelial voltohmmeter (World Precision Instruments, Sarasota, FL, USA). Readings were taken of RBE4-only seeded Transwell insert and RBE4/C6 Transwell BBB model, and were compared to collagen-coated Transwell inserts (no cells) used as a blank control; readings were carried out in triplicate ($n=3$).

RESULTS

Characterization of Glutathione-Coated PEGylated PLGA NP

Microtrac FLEX (Microtrac Inc., PA, USA) was used to analyze the particle sizes of docetaxel NP through dynamic light scattering. Three samples of the docetaxel NP suspension were analyzed ($n=3$). The median size of the docetaxel nanoparticle was found to be 374.25±38.95 nm, possibly due to aggregation. Microtrac FLEX software also analyzes the average size of NPs by focusing on smaller, nonaggregated NPs and found that the average size of particles was 83.76±7.66 nm. The same software was used to measure the zeta potential of the NPs ($n=3$). The zeta potential of the same nanoparticles was found to be −22.38±14.73 mv (mean value±SE).

Determination of Entrapment Efficiency

UV spectroscopy analysis at a wavelength of 231 nm (λ_{max}) was used to analyze the UV absorbance of docetaxel NPs in methanol as compared to standard curve of docetaxel solubilized in methanol ($r^2=0.9971$). Spectroscopy analysis revealed the entrapment efficiency of docetaxel by PEGylated PLGA NPs to be 27.70±0.38%.

In Vitro Drug Release

In vitro drug release data of docetaxel NPs in PBS is shown by Fig. 1 as the percentage of docetaxel released over 240 h (10 days). Approximately 18.49±5.21% of the drug was released in 240 h. There is a slight burst release of the drug from the nanoparticle in the first 24 h, followed by a sustained release of the drug for the remainder of the time period investigated.

MTT Assay

Cytotoxicity data of docetaxel drug solution, docetaxel NP, and GSH-coated docetaxel NP treatments in C6 cells is shown by Fig. 2. Figure 2 compares the cytotoxicity data of the

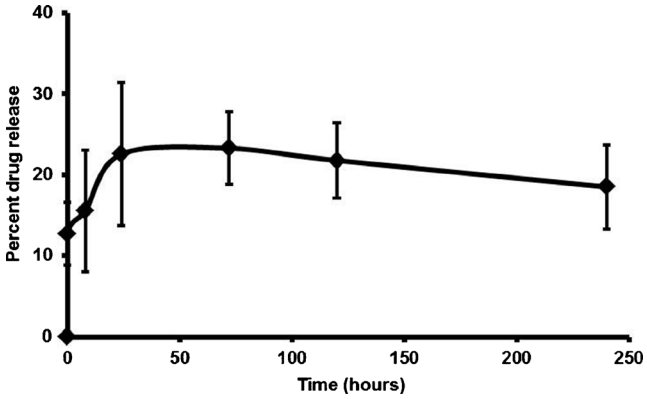

Fig. 1 *In vitro* drug release data of docetaxel-loaded nanoparticles in 10-mL PBS release buffer. Samples were analyzed by UV spectroscopy (λ_{max}, 231 nm) at predetermined intervals. *Graph* represents mean percentage of drug released over 240 h in triplicate ($n=3$)±SD

following treatments: 5 μM free docetaxel drug solution, 5 μM docetaxel NP, and 5 μM GSH-coated docetaxel NP with 10 μM free docetaxel drug solution, 10 μM docetaxel NP, and 10 μM GSH-coated docetaxel NP. All three treatments of 5 μM were cytotoxic as compared to untreated cells, approximately 70% viability in 5 μM free docetaxel drug solution, 51% in 5 μM docetaxel NP, 38% in 5 μM GSH-coated docetaxel NP. All three treatments of 10 μM were cytotoxic as compared to untreated cells, approximately 74% viability in 10 μM free docetaxel drug solution, 47% in 10 μM docetaxel nanoparticle, and 15% in 10 μM GSH-coated docetaxel nanoparticle.

Cytotoxicity data of docetaxel drug solution, docetaxel NP, and GSH-coated docetaxel NP treatments in RG2 cells is shown by Fig. 3. Figure 3 compares the cytotoxic data of the following treatments: 5 μM free docetaxel drug solution, 5 μM docetaxel NP, and 5 μM GSH-coated docetaxel NP with 10 μM free docetaxel drug solution, 10 μM docetaxel NP, and 10 μM GSH-coated docetaxel NP. All three treatments

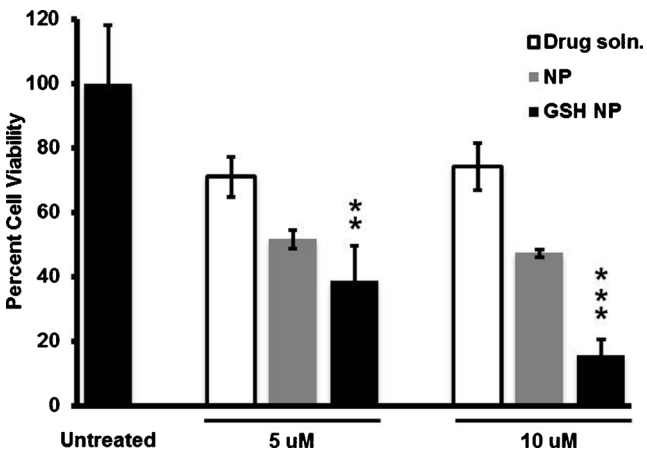

Fig. 2 MTT assay in C6 cells of untreated cells *versus* treatments of free docetaxel drug solution, docetaxel-loaded nanoparticles, and GSH-coated docetaxel-loaded nanoparticles (5 *vs.* 10 μM treatments of each). Treatments were carried out in triplicates ($n=3$) and the data represents the mean cellular viabilities±SD. Results were quantified using a Synergy H4 plate reader (Biotek Industries Inc.) at absorbance of 570 nm. Statistical analysis was carried out using paired *t* tests ($p \leq 0.01$)

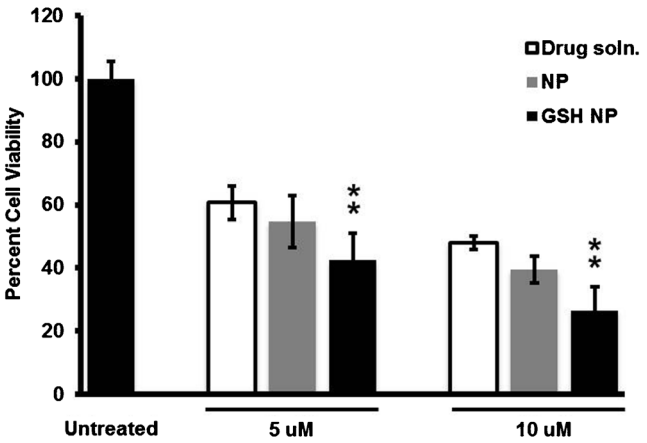

Fig. 3 MTT assay in RG2 cells of untreated cells *versus* treatments of free docetaxel drug solution, docetaxel-loaded nanoparticles, and GSH-coated docetaxel-loaded nanoparticles (5 *vs.* 10 μM treatments of each). Treatments were carried out in triplicates ($n=3$) and the data represents the mean cellular viabilities±SD. Results were quantified using a Synergy H4 plate reader (Biotek Industries Inc.) at absorbance of 570 nm. Statistical analysis was carried out using paired *t* test ($p \leq 0.01$)

of 5 μM were found to be more cytotoxic as compared to untreated cells, approximately 61% viability for free docetaxel drug solution, 55% for docetaxel NP, and 43% for GSH-coated docetaxel NP. All three treatments of 10 μM were found to be more cytotoxic as compared to untreated cells, approximately 48% viability for free docetaxel drug solution, 40% for docetaxel NP, and 27% for GSH-coated docetaxel NP.

Paired *t* test statistical analyses comparing the docetaxel-free drug solution with GSH-coated NPs (both 5 and 10 μM) in C6 and RG2 cells showed that the GSH-coated NPs were

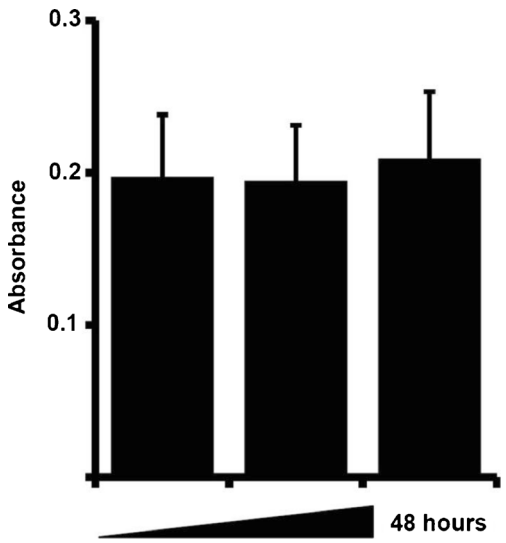

Fig. 4 Trans-BBB permeation data of 5 μM GSH-coated docetaxel-loaded nanoparticles across Transwell™ permeable supports seeded with RBE4 and C6 cells. One hundred-microliter samples of media were taken from under the permeable support at predetermined intervals and replaced with fresh media. Media samples were analyzed by UV spectroscopy at absorbance of 231 nm (λ_{max}). Treatment of cells was carried out in triplicate ($n=3$) and represented data shows mean absorbance±SD

Table I. TEER Values Obtained over a 2-Day Period of RBE4-Only Culture and RBE4/C6 Culture on Transwell Permeable Support

	DAY 1	DAY 2
RBE4 ONLY	99.68 ± 0 Ω cm^2	120.21 ± 25.25 Ω cm^2
RBE4/C6	144.48 ± 0 Ω cm^2	168.75 ± 23.31 Ω cm^2

Values are reported as mean resistance of triplicate (n = 3) ± SD. TEER values were measured using the STX2 electrode and EVOM^2 epithelial voltohmmeter (World Precision Instruments, Sarasota, FL, USA)

significantly better in killing both glioma model cells than the docetaxel-free drug solution.

In Vitro Blood–Brain Barrier Permeation Model

UV–Vis spectroscopy (231 nm, λ_{max}) was used to analyze media samples taken from Transwell *in vitro* BBB model for GSH-coated docetaxel NP at predetermined intervals. The data of the UV absorbance data is presented by Fig. 4. At all points, the permeation of 5 μM GSH-coated docetaxel NPs was greater than that of 5 μM free docetaxel drug solution (data not shown). The permeation rate across the tested time ranges (16–48 h) seems to be consistent.

Trans-Endothelial Electrical Resistance of the Transwell Model

The results of TEER measurements for RBE4-only and RBE4/C6 inserts are shown in Table I. The resistance of the RBE4/C6 inserts was found to be greater than the RBE4-only insert at both time points tested. At day 1, the resistance of the RBE-4 only insert was found to be 99.68±0 Ω cm^2 for RBE4-only and 144.48±0 Ω cm^2 for RBE4/C6. At day 2, the resistance of the RBE-4 only insert was found to be 120.21± 25.25 Ω cm^2 and 168.75±23.31 Ω cm^2 for RBE4/C6.

DISCUSSION

Dynamic light scattering was used to analyze the size of the NPs. Although the median particle size tested by the Microtrac FLEX machine was a rather large median size for NPs (374.25±38.95 nm), this was assumed to be attributed to clumping. The average size obtained through the Microtrac FLEX software that focuses on the smaller particles reflects a more accurate representation of the individual NPs in solution (83.76±7.66 nm). As previously reported by us, coating the particles with GSH would slightly increase the average size of the NPs but not by a considerable amount (10,11; Fig. 5). The average size of NPs was found to be compatible with the size of NPs that are able to permeate the BBB (27). The zeta potential of the NPs was found to be −22.38±14.73 mv using Microtrac FLEX. The zeta potential reveals moderate stability in solution, but suggests that there would be some aggregation of the NPs in solution. The negative charge associated with the NPs suggests that the coating of GSH onto the NP surface may occur through an electrostatic interaction between the charge of GSH and the charge on the surface of the NPs. In addition, the negative charge associated with the NPs may suggest its extended suspension in the blood to allow for its permeation across the BBB (28).

GSH was coated onto the docetaxel NPs after their formation by the nanoprecipitation method, leading to the assumption that coating the particles with GSH would not greatly affect the encapsulation of the drug. The encapsulation of the docetaxel drug by the NP polymer during the nanoprecipitation method is thought to be driven by the hydrophobic interactions of nonpolar moieties on the docetaxel drug with the lipid chains of the NP polymer.

In vitro release data of docetaxel NPs in PBS reveals that approximately 18.5% of the drug is released over a 10-day period. The slight burst release of the drug could be due to a small amount of the drug existing on the surface of the NP, a remnant of the nanoprecipitation process. A 15-μM solution was chosen for the study due to the low aqueous solubility. The drug exhibits a sustained release from the PLGA polymer over the 10-day period (23).

In the MTT assay data obtained from C6 cells, there seemed to be consistent cell viabilities in free docetaxel drug solution and docetaxel NP treatments across both treatment concentrations (5 and 10 μM). However, there was an excess of twofold decrease in cell viability in GSH-coated docetaxel NP treatments in 10-μM treatment as compared to the 5-μM treatment. The lower cell viabilities in GSH-coated docetaxel NP treatments in C6 cells across both treatment concentrations

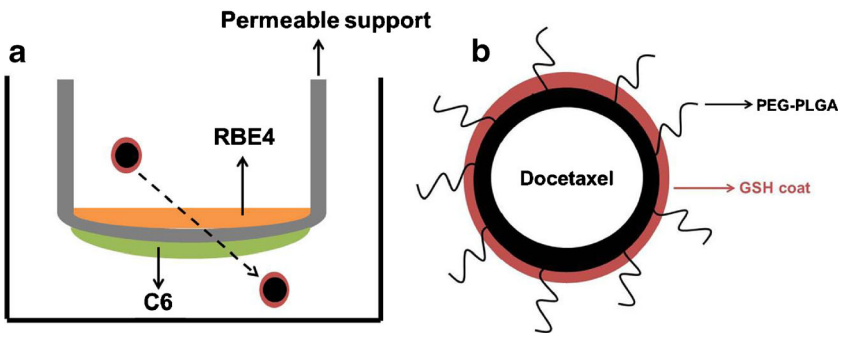

Fig. 5 **a** Graphical representation of Transwell™ model established through co-culturing RBE4 cells with C6 cells. **b** Graphical representation of docetaxel drug encapsulated by PEGylated PLGA nanoparticle due to hydrophobic interactions between nonpolar moieties on docetaxel and PEGylated PLGA lipid chains. The GSH coat exists outside of the nanoparticle and may slightly increase the particle's size without affecting the entrapment efficiency of the drug

(as compared to free docetaxel drug solution and docetaxel NP treatments) reveals that GSH-coated docetaxel NPs were more effective in killing C6 astrocytoma cells than free docetaxel drug solution and docetaxel NP treatments. In both 5- and 10-μM treatments in the C6 cell line, GSH-coated docetaxel NPs were significantly better at killing C6 cells than the free docetaxel drug solution ($p \leq 0.01$). However, in RG2 cells, there was a visible, dose-dependent decrease in cellular viability when comparing respective treatments between 5- and 10-μM treatments. The decrease in viabilities was less than twofold when comparing free docetaxel drug solution and docetaxel NP treatments between 5- and 10-μM treatments, but there was a twofold decrease in RG2 cell viability in GSH-coated docetaxel NP treatments between 5- and 10-μM treatments. In both treatment sets (5 and 10 μM), GSH-coated docetaxel NPs were better inducers of cell death in the RG2 glioma model. In both 5- and 10-μM treatments in the RG2 cell line, GSH-coated docetaxel NPs were significantly better at killing RG2 cells than the free docetaxel drug solution ($p \leq 0.01$).

We have previously shown that the PLGA-based NP vector is safe for cellular use and does not impair basic cellular activities of RG2 cells (10,11). We anticipate the same, low-toxic effect of the PLGA vector in the RG2 and C6 cells used in this study. In the present study, we show through MTT tests that the docetaxel drug released from the GSH-coated NPs induces cell death in the C6 and RG2 glioma cell lines better than the free docetaxel drug solution, suggesting their use as a possible brain-targeted anti-mitotic therapy. In addition, paired *t* test analyses show that GSH-coated docetaxel-loaded NPs were significantly better in inducing glioma cell death as compared to the free drug solution in all treatments, indicating that the GSH-coated NP form of the drug is more efficient than the free drug solution for clinical use. We attribute the decreased cell viabilities from GSH-coated docetaxel NPs across the board to be due to a greater cellular internalization of the NPs by the C6 and RG2 cells, which can be attributed to the GSH coat on the docetaxel NPs.

Data obtained from the Transwell™ model revealed that trans-BBB permeation over the 48 h tested seems to be constant, suggesting that the permeation of GSH-coated docetaxel NPs seems to be time-dependent within the first 16 h of cellular treatment. However, further studies would be necessary to ascertain this. UV absorbance data of trans-BBB permeation of GSH-coated docetaxel NP reinforces the initial hypothesis that GSH-coated NPs are able to permeate the BBB.

Testing the TEER of the Transwell BBB model allowed us to validate the effectiveness of our model. The resistance of the RBE4/C6 BBB Transwell model was compared to a RBE-4 only Transwell monoculture to investigate whether the interaction of RBE4 cells with C6 astrocytes induces the formation of tight junctions as proposed *in vivo* situations. It was found that the TEER values of the RBE4/C6 model was greater than that of RBE-4 only over the 2-day period tested, revealing that the interaction of the endothelial cells with astrocytes induces a greater tightness in the Transwell model than the endothelial cell monoculture. Although the TEER values obtained by the Transwell cultures are much less than those values exhibited *in vivo* situations (1,500–2,000 Ω cm^2), they are consistent with TEER values obtained by human cerebral microvascular endothelial cells (hCMEC; 20–200 Ω cm^2) (19). The hCMEC/D3 cell line is considered one of the foremost cell lines to retain the expression of junctional proteins consistent with BBB physiology (29). However, TEER values obtained through mono-, co-, and tri-cultures of hCMEC/D3 cells with human cerebral astrocytes (CC-2565 cell line) and human vascular pericytes (HBVP) revealed lower TEER values over 2 days (ranging from approximately 32–60 Ω cm^2) than RBE4-only and RBE4/C6 model TEER values reported by us in the present study (19).

Brain-related disorders are the hardest to treat due to the obstruction caused by the BBB. Although it is effective in protecting the brain from toxins and other compounds that may be potentially harmful to neural tissue, the BBB also restricts neural access to compounds that could be therapeutic. By utilizing the existing GSH transport mechanism in the brain, GSH-coated docetaxel-loaded NPs can be a novel therapy in battling the aggressiveness of gliomas, as has been previously reported by us using GSH-coated paclitaxel NPs in C57BL/6 mice, showing that GSH-coated NPs are able to permeate the BBB after being injected peritoneally (10). This is one of the first studies to propose the use of docetaxel as an anti-brain cancer agent. Docetaxel has been used as an anti-mitotic agent in a number of different cancers but has not been used in the brain due to the difficulty of surmounting the BBB. The present study hypothesizes the coating of docetaxel-loaded, PLGA NP with GSH to enhance the trans-BBB permeation (Fig. 5).

CONCLUSION

BBB permeation data obtained from a Transwell *in vitro* BBB model revealed that GSH-coated docetaxel NPs were able to permeate the BBB better than the free docetaxel drug solution. MTT assays in RG2 and C6 cells, both glioma models, showed that docetaxel-encapsulated PLGA NPs were not overly toxic to cells and revealed cell death in the glioma models, suggesting the drug's use in brain cancers as an anti-mitotic agent. In addition, MTT data suggests that docetaxel-encapsulated PLGA NPs are a safe vector against brain cancers and are effective in reducing cell viability through the release of the docetaxel therapeutic compound from the PLGA NPs. As shown by the *in vitro* drug release data, the drug exhibited a sustained release from the NP vector and was very well encapsulated by the NP with low residue on the surface, suggesting that the NP form of the drug is a safe method by which to administer the drug, reducing the side effects caused by the free drug. Taken together along with the Transwell data, we suggest that docetaxel in this form could be used effectively in clinical settings against brain cancers.

REFERENCES

1. Yared JA, Tkaczuk KH. Update on taxane development: new analogs and new formulations. Drug Des Dev Ther. 2012;6:371.
2. Tije AJ, Verweij J, Loos WJ, Sparreboom A. Pharmacological effects of formulation vehicles: implications for cancer chemotherapy. Clin Pharmacokinet. 2003;42(7):665–85.
3. Sanson M, Napolitano M, Yaya R, Keime-Guibert F, Broët P, Hoang-Xuan K, *et al*. Second line chemotherapy with docetaxel in patients with recurrent malignant glioma: a phase II study. J Neuro-Oncol. 2000;50(3):245–9.

4. Kleihues P, Cavenee W. Pathology and genetics of tumours of the nervous system. International Agency for Research on Cancer (IARC) and WHO Health Organisation. Oxford: Oxford Press; 2000.
5. Lefranc F, Sauvage S, Van Goietsenoven G, Mégalizzi V, Lamoral-Theys D, Debeir O, *et al.* Narciclasine, a plant growth modulator, activates Rho and stress fibers in glioblastoma cells. Mol Cancer Ther. 2009;8(7):1739–50.
6. Lefranc F, Brotchi J, Kiss R. Possible future issues in the treatment of glioblastomas: special emphasis on cell migration and the resistance of migrating glioblastoma cells to apoptosis. J Clin Oncol. 2005;23(10):2411–22.
7. Grobben B, De Deyn P, Slegers H. Rat C6 glioma as experimental model system for the study of glioblastoma growth and invasion. Cell Tissue Res. 2002;310(3):257–70.
8. Kleihues P, Ohgaki H. Primary and secondary glioblastomas: from concept to clinical diagnosis. Neuro-Oncology. 1999;1(1):44–51.
9. Benda P, Lightbody J, Sato G, Levine L, Sweet W. Differentiated rat glial cell strain in tissue culture. Science. 1968;161(3839):370–1.
10. Geldenhuys W, Mbimba T, Bui T, Harrison K, Sutariya V. Brain-targeted delivery of paclitaxel using glutathione-coated nanoparticles for brain cancers. J Drug Target. 2011;19(9):837–45.
11. Carroll RT, Bhatia D, Geldenhuys W, Bhatia R, Miladore N, Bishayee A, *et al.* Brain-targeted delivery of Tempol-loaded nanoparticles for neurological disorders. J Drug Target. 2010;18(9):665–74.
12. Cecchelli R, Berezowski V, Lundquist S, Culot M, Renftel M, Dehouck M-P, *et al.* Modelling of the blood–brain barrier in drug discovery and development. Nat Rev Drug Discov. 2007;6(8):650–61.
13. Meyers JD, Doane T, Burda C, Basilion JP. Nanoparticles for imaging and treating brain cancer. Nanomedicine. 2013;8(1):123–43.
14. Kuhnline Sloan CD, Nandi P, Linz TH, Aldrich JV, Audus KL, Lunte SM. Analytical and biological methods for probing the blood–brain barrier. Annu Rev Anal Chem. 2012;5:505–31.
15. Valdovinos-Flores C, Gonsebatt ME. The role of amino acid transporters in GSH synthesis in the blood–brain barrier and central nervous system. Neurochem Int. 2012;61(3):405–14.
16. Limón-Pacheco JH, Hernández NA, Fanjul-Moles ML, Gonsebatt ME. Glutathione depletion activates mitogen-activated protein kinase (MAPK) pathways that display organ-specific responses and brain protection in mice. Free Radic Biol Med. 2007;43(9):1335–47.
17. Gaillard PJ. Glutathione-based drug delivery system. Google Patents; 2010.
18. Cecchelli R, Dehouck B, Descamps L, Fenart L, Buée-Scherrer V, Duhem C, *et al.* In vitro model for evaluating drug transport across the blood–brain barrier. Adv Drug Deliv Rev. 1999;36(2):165–78.
19. Hatherell K, Couraud P-O, Romero IA, Weksler B, Pilkington GJ. Development of a three-dimensional, all-humanin vitromodel of the blood–brain barrier using mono-, co-, and tri-cultivation Transwell models. J Neurosci Methods. 2011;199(2):223–9.
20. Gaillard PJ, Voorwinden LH, Nielsen JL, Ivanov A, Atsumi R, Engman H, *et al.* Establishment and functional characterization of an in vitro model of the blood–brain barrier, comprising a co-culture of brain capillary endothelial cells and astrocytes. Eur J Pharm Sci. 2001;12(3):215–22.
21. Garcia CM, Darland DC, Massingham LJ, D'Amore PA. Endothelial cell–astrocyte interactions and TGFβ are required for induction of blood–neural barrier properties. Dev Brain Res. 2004;152(1):25–38.
22. Sah H, Thoma LA, Desu HR, Sah E, Wood GC. Concepts and practices used to develop functional PLGA-based nanoparticulate systems. Int J Nanomedicine. 2013;8:747.
23. Danhier F, Ansorena E, Silva JM, Coco R, Le Breton A, Préat V. PLGA-based nanoparticles: an overview of biomedical applications. J Control Release. 2012;161(2):505–22.
24. Owens III DE, Peppas NA. Opsonization, biodistribution, and pharmacokinetics of polymeric nanoparticles. Int J Pharm. 2006;307(1):93–102.
25. Sabzevari A, Adibkia K, Hashemi H, Hedayatfar A, Mohsenzadeh N, Atyabi F, *et al.* Polymeric triamcinolone acetonide nanoparticles as a new alternative in the treatment of uveitis: In vitro and in vivo studies. Eur J Pharm Biopharm. 2013;84(1):63–71.
26. Etame AB, Smith CA, Chan WC, Rutka JT. Design and potential application of PEGylated gold nanoparticles with size-dependent permeation through brain microvasculature. Nanomedicine: NBM. 2011;7(6):992–1000.
27. Hatakeyama H, Akita H, Maruyama K, Suhara T, Harashima H. Factors governing the in vivo tissue uptake of transferrin-coupled polyethylene glycol liposomes in vivo. Int J Pharm. 2004;281(1):25–33.
28. Jinwal U, Groshev A, Zhang J, Grover A, Sutariya V. Preparation and Characterization of Methylene blue Nanoparticles for Alzheimer's disease and other Tauopathies. Curr Drug Deliv. 2013.
29. Wilhelm I, Fazakas C, Krizbai IA. In vitro models of the blood–brain barrier. Acta Neurobiol Exp (Wars). 2011;71(1):113–28.